




ESA Climate Change Initiative – Fire_cci

D2.1.4 Algorithm Theoretical Basis Document (ATBD) – Small Fires Dataset (SFD)

Project Name	ECV Fire Disturbance: Fire_cci
Contract N°	4000126706/19/I-NB
Issue Date	03/11/2021
Version	1.0
Author	Ekhi Roteta
Document Ref.	Fire_cci_D2.1.4_ATBD_SFD_v1.0
Document type	Public

To be cited as: Roteta E. (2021) ESA CCI ECV Fire Disturbance: D2.1.4 Algorithm Theoretical Basis Document-SFD, version 1.0. Available at: <https://climate.esa.int/en/projects/fire/key-documents/>

	Fire_cci	Ref.:	Fire_cci_D2.1.4_ATBD_SFD_v1.0		
	Algorithm Theoretical Basis	Issue	1.0	Date	03/11/2021
	Document – Small Fires Dataset	Page			2


Project Partners

Prime Contractor/ Scientific Lead & Project Management	UAH – University of Alcalá (Spain)
Earth Observation Team	UAH – University of Alcalá (Spain)
	UPM – Universidad Politécnica de Madrid (Spain) CNR-IREA - National Research Council of Italy – Institute for Electromagnetic Sensing of the Environment (Italy)
System Engineering	BC – Brockmann Consult (Germany)
Climate Modelling Group	MPIM – Max Planck Institute for Meteorology (Germany)
	CNRS - National Centre for Scientific (France)



Distribution

Affiliation	Name	Address	Copies
ESA	Clément Albergel (ESA)	clement.albergel@esa.int	electronic copy
Project Team	Emilio Chuvieco (UAH)	emilio.chuvieco@uah.es	electronic copy
	M. Lucrecia Pettinari (UAH)	mlucrecia.pettinari@uah.es	
	Joshua Lizundia (UAH)	joshua.lizundia@uah.es	
	Amin Khaïroun (UAH)	amin.khairoun@uah.es	
	Gonzalo Otón (UAH)	gonzalo.oton@uah.es	
	Mihai Tanase (UAH)	mihai.tanase@uah.es	
	Consuelo Gonzalo (UPM)	consuelo.gonzalo@upm.es	
	Dionisio Rodríguez Esparragón (UPM)	dionisio.rodriguez@ulpgc.es	
	Ángel García Pedrero (UPM)	angelmario.garcia@upm.es	
	Daniela Stroppiana (CNR)	stroppiana.d@irea.cnr.it	
	Mirco Boschetti (CNR)	boschetti.m@irea.cnr.it	
	Carsten Brockmann (BC)	carsten.brockmann@brockmann-...	
	Thomas Storm (BC)	thomas.storm@brockmann-consult.de	
	Martin Böttcher (BC)	martin.boettcher@brockmann-cons...	
Angelika Heil (MPIM)	angelika.heil@mpimet.mpg.de		
Idir Bouarar (MPIM)	idir.bouarar@mpimet.mpg.de		
Florent Mouillot (CNRS)	florent.mouillot@cefe.cnrs.fr		
Philippe Ciais (CNRS)	philippe.ciais@lsce.ipsl.fr		

	Fire_cci		Ref.:	Fire_cci_D2.1.4_ATBD_SFD_v1.0		
	Algorithm Theoretical Basis		Issue	1.0	Date	03/11/2021
	Document – Small Fires Dataset		Page	3		

Summary

This document describes the algorithm used for generating the small-fire dataset version 2.0 within the Fire_cci project, with data from the MSI sensor on board the Sentinel-2 A&B satellites.

	Affiliation/Function	Name	Date
Prepared	EHU	Ekhi Roteta	03/11/2021
Reviewed	UAH – Project Manager	Lucrecia Pettinari	03/11/2021
Authorized	UAH - Science Leader	Emilio Chuvieco	03/11/2021
Accepted	ESA - Technical Officer	Clément Albergel	

This document is not signed. It is provided as an electronic copy.

Document Status Sheet

Issue	Date	Details
0.1	01/05/2017	Internal draft release of the document.
1.0	01/10/2018	First public release of the document
D2.1.4 v1.0	03/11/2021	Release corresponding to FireCCISFD20

Document Change Record

Issue	Date	Request	Location	Details
1.0	01/10/2018	UAH ESA ESA ESA, UL ESA UL ESA ESA UL UAH, UL ESA-UL	All document Section 3 Sections 4.1 and 4.2 Section 4.2 Section 4.3, 4.6.4, 4.6.8, 5.1 Sections 4.5, 5.2 Section 4.6.3 Section 4.6.7 Figure 14 Section 4.6.9 Section 6	Removed references to the S-1 algorithm, which are included in a separate document, and Landsat-8 tests. Text expanded. Sections merged and text reduced. The previous section 4.6 was moved to section 4.2 and expanded. Small changes in the text. Sections updated. Text expanded. Clarification added on threshold selection. Figure updated. New section added. Text expanded, and merged with previous Section 7
D2.1.4 v1.0	03/11/2021	EHU UAH	General Sections 1, 2.1, 4.3.1.1, 4.3.2 Section 2.3, previous sections 4.3, 4.4, 4.5.1.1, 4.5.1.2 Sections 3 Sections 4.1, 4.2, 4.3.1, 4.3.5, 5, 6, 7 Section 4.3.10	Change of the number of the deliverable Small updates in the text Sections removed Sections expanded Sections updated Section added


	Fire_cci	Ref.:	Fire_cci_D2.1.4_ATBD_SFD_v1.0		
	Algorithm Theoretical Basis Document – Small Fires Dataset	Issue	1.0	Date	03/11/2021
		Page	4		

Table of Contents

2	Executive Summary	6
3	Introduction.....	6
3.1	Background.....	6
3.2	Purpose of the document.....	7
4	The Small Fire Dataset	7
5	Data and Methods	8
5.1	Sentinel-2 products	8
5.2	Active fire products	9
5.3	Classification of Burned and Non-Burned Vegetation	9
5.3.1	Preparation of data.....	9
5.3.2	General overview of the BA algorithm	11
5.3.3	Not burnable mask.....	13
5.3.4	Initially Burned/Not Burned Area detection (IB/INB).....	14
5.3.5	Initially Burned (Not) Confirmed (IBC/IBNC).....	14
5.3.6	Burned seeds.....	15
5.3.7	Second Stage Probability of Burn (SEPB)	15
5.3.8	Probability of burn results	17
5.3.9	Resampling of the Probability of burn	18
5.3.10	Merging of Sentinel-2A and -2B	19
6	Results of Test over the study areas	21
7	Limitations of the product.....	23
8	References	23
	Annex: Acronyms and abbreviations	25

List of Tables

Table 1.	Rules applied to obtain the not burnable mask.....	13
Table 2.	Rules applied to obtain the Initially Burned Result	14
Table 3.	Rules applied to obtain Burned Seeds	15
Table 4.	Lookup Table for the rescaling process.....	19
Table 5.	Quality assessment of the SFD algorithm in the 26 test areas.	22

List of Figures

Figure 1.	Reference perimeters and validation results, using only S2A data or both S2A and S2B images, in a sample area in tile 36LWN.	9
Figure 2.	Compositing of two images of the same date in the 33PTK study area of both false colour SWIR2-NIR-Red image and SCL (the right column is the compositing result).....	10
Figure 3.	Aggregation process for the Sentinel 2 images from a single satellite	11
Figure 4.	BA algorithm for each pair of Images considered	13


	fire cci	Fire_cci		Ref.:	Fire_cci_D2.1.4_ATBD_SFD_v1.0		
		Algorithm Theoretical Basis		Issue	1.0	Date	03/11/2021
		Document – Small Fires Dataset		Page	5		

Figure 5. s-shape and z-shape sigmoid membership functions applied to MIRBI and NBR2 temporal differences, in tile 28PET between December 22 2015 and January 11 2016. 16


Figure 6. Extension of seeds’ influence area in the SEPB for a sample zone of the 30PWQ study area, between 27th December 2015 and 6th January 2016; the legend is the same for all the maps. 18

Figure 7. Evolution of omission and commission errors depending on the threshold in two sample tiles (31PEN to the left and 34PET to the right). 19

Figure 8. Comparison of a BAS2A P_b image with closest previous and next BAS2B images, and removal of BA that were not detected by BAS2B. 20

Figure 9. Comparison of errors depending on the datasets used or how these datasets are combined, in the same sample area as Figure 11. 21

Figure 10. Location of the 26 test sites and major Olson biomes. 21

	<p style="text-align: center;">Fire_cci Algorithm Theoretical Basis Document – Small Fires Dataset</p>	Ref.:	Fire_cci_D2.1.4_ATBD_SFD_v1.0			
		Issue	1.0	Date	03/11/2021	
		Page				6

2 Executive Summary

Fires emit greenhouse gases (GHGs) and aerosols, important climate forcing factors, which need to be estimated and modelled to better understand climate and carbon cycling. Fires are also a major factor in land cover change, and hence affect fluxes of energy and water to the atmosphere. In this context, spatial and temporal monitoring of trace gas emissions from fires is of primary importance. These can be inferred using both land-surface and atmospheric measurements, preferably in combination. The Fire Disturbance Essential Climate Variable provides baseline products for the land-surface to allow this.

Burned area (BA), as derived from satellites, is considered the primary variable that requires climate-standard continuity. It can be combined with information on burn efficiency and available fuel load to estimate emissions of trace gases and aerosols. Measurements of BA may be used as direct input (driver) to climate and carbon cycle models or, when long time series of data are available, to parameterise climate-driven models for BA (GCOS, 2016).

This document is the Algorithm Theoretical Basis Document (ATBD) corresponding to the generation of the small fires dataset for the year 2019. It describes the algorithm method and approach that has led to the generation of the small fire dataset for the continent of Africa, named FireCCISFD20, which contains fires burned in 2019 and follows the previous SFD called FireCCISFD11 with fires from 2016 in the same area. The theoretical basis described here identifies the data sets that were used to classify burned area and the methods used to derive the BA products.


3 Introduction

3.1 Background

The ESA CCI initiative stresses the importance of providing a higher scientific visibility to data acquired by ESA sensors, especially in the context of the IPCC reports. This implies to produce consistent time series of accurate Essential Climate Variables (ECV) products, which can be used by the climate, atmospheric and ecosystem scientists for their modelling efforts. The importance of keeping long-term observations and the international links with other agencies currently generating ECV data is also stressed.

The fire disturbance ECV identifies BA (BA) as the primary fire variable. Accordingly, the Fire_cci project shall focus on developing and validating algorithms to meet GCOS ECV requirements for (consistent, stable, error-characterised) global satellite data products from multi-sensor data archives.

All global BA products are based on coarse resolution sensors (from 250 to 1000m). Therefore, the likelihood of detecting small burns (i.e. < 50ha) is very low, and therefore omission errors from these products may be quite high (Padilla et al., 2015; Giglio et al., 2009), particularly coming from small fires (Randerson et al., 2012). In order to improve the characterisation of small fires, one of the objectives of the project is to generate a small fires dataset based on medium resolution sensors (10 to 100m). Considering the huge processing effort to cover the whole planet, this SFD shall be focused on the African continent, which is the most burned worldwide (Chuvienco et al, 2016; Giglio et al., 2013). The first SFD, named FireCCISFD11, was generated within the Phase 2 of the Fire_cci project and contained areas burned in 2016 in Sub-Saharan Africa (Roteta et al., 2019). This second SFD, now called FireCCISFD20, has been generated in the same region but for fires burned in 2019.

 fire cci	Fire_cci	Ref.:	Fire_cci_D2.1.4_ATBD_SFD_v1.0		
	Algorithm Theoretical Basis Document – Small Fires Dataset	Issue	1.0	Date	03/11/2021
		Page			7

3.2 Purpose of the document

This document describes the algorithm theoretical basis from which to map burned areas from moderate resolution optical data. It further provides initial results of a mapping exercise in specially selected test sites in Africa.

4 The Small Fire Dataset


Burned Area (BA) is defined in this document as any vegetated area that has been completely or partially consumed by a fire, regardless of whether that fire was human or natural causes, or whether that fire affected wildland areas or human managed territories (agricultural or pastures).

Since several coarse-resolution burned area detection algorithms require that a substantial fraction of an individual pixel's area undergo burning for successful attribution (to avoid commission errors from other forms of land cover change), detection of small fires becomes difficult (Roy and Landmann 2005). At a global scale, it has been shown that accounting for small fires may increase burned area and global carbon emissions by approximately 35% (Randerson et al. 2012). The small fire dataset will be used to establish whether the estimate by Randerson et al. can be verified (using a continental data set as a first indicator) and address what the contribution of small fires might be.

It is known that the strategy of using active fire products may provide new information on small fire contribution to burned area and emissions because of the strong nonlinearity in radiative power as a function of fire temperature. Active fires have shown very low commission errors, but very diverse omission rates depending on the ecosystem and fire size (36–86%), the detection of those below 500 ha is quite high (omissions < 20%) (Hantson et al. 2013). Given this context, there is a real need to link coarse resolution products with data on small burned patches, in particular in locations where these are the dominant fire types (e.g. sub-Saharan Africa). This could be achieved with higher resolution remote sensing data such as Landsat-OLI (30 m) or Sentinel-2 optical data (10 m).

The capability of Landsat TM and ETM+ data to provide information on burned scars has been widely recognized in scientific literature due to its spatial coverage, medium spatial resolution, multispectral characteristics (covering the most important spectral areas for burned area mapping with one band in the near infrared and two in the shortwave infrared) and specially for the historical dataset, with data available since 1982 until now (the last satellite, Landsat-8, was launched in 2013). Although some local/regional burned area algorithms based on Landsat TM/ETM images have been developed (Bastarrika et al. 2014; Bastarrika et al. 2011b; Chuvieco et al. 2002), recent developments have shown the potential of these sensors even for global BA products. Obviously, global BA algorithms are much more challenging than local based, as the proposals by the USGS (http://remotesensing.usgs.gov/ecv/BA_overview.php, last accessed July 2018) and Boschetti et al. (2015) have shown. For both, only some partial validation results have been published.

One of the most critical issues in Landsat is the temporal resolution (16 days), not enough for tropical ecosystems where the vegetation recovers very fast. This issue is improved with the Sentinel-2 mission, which allows a high revisit frequency (5 days at the equator when the Sentinel 2A and 2B satellites are working simultaneously). The Multi Spectral Instrument (MSI) that is carried by these satellites provides a unique combination of high spatial resolution (which varies from 10 m to 20 m), a wide field of view (290 km) and

 fire cci	Fire_cci		Ref.:	Fire_cci_D2.1.4_ATBD_SFD_v1.0		
	Algorithm Theoretical Basis		Issue	1.0	Date	03/11/2021
	Document – Small Fires Dataset		Page	8		

spectral coverage (13 spectral bands spanning from the visible and the near infrared to the short wave infrared), and represents a major step forward compared to current multi-spectral missions (Drusch et al. 2012).

The first version of the SFD, called FireCCISFD11, detected areas burned in 2016 in sub-Saharan Africa from Sentinel-2A images at 20 m (Roteta et al., 2019). With lower errors than global products at coarse resolution (commissions and omissions of 19.3% and 26.5%, respectively), 4.9 M km² of BA were detected in total by FireCCISFD11, which meant an increase of 54% if compared with FireCCI51 (3.2 M km² in sub-Saharan Africa in 2016), or 80% with MCD64A1 (2.7 M km²).

This second version of the SFD, called FireCCISFD20, covers the same area in sub-Saharan Africa at the same spatial resolution, but detects areas burned in 2019. The main differences are the inclusion of images acquired by both Sentinel-2A and Sentinel-2B satellites, improving the revisit time from 10 to 5 days, and the replacement of the MCD14DL product with VIIRS active fires, which have a higher spatial resolution of 375 m (vs. 1 km for MODIS hotspots). Both Sentinel-2B images and VIIRS active fires were not available yet when the previous FireCCISFD11 was developed.


5 Data and Methods

5.1 Sentinel-2 products

The data used for this newer version of the SFD in 2019 (FireCCISFD20) are the Sentinel-2 MSI Level-2A product, which contains Bottom-of-atmosphere (BOA) reflectances and a Scene Classification (SCL) projected in UTM WGS84 system. This Level-2A product was created from Level-1C data using the ESA processor Sen2Cor at CreODIAS. For the older SFD in 2016 (FireCCISFD11) the Level-1C product with Top-of-atmosphere (TOA) reflectances was downloaded from the Copernicus Open Access Hub, and the Level-2A product was generated by the Sentinel-2 ESA toolbox at the beginning of the BA classification. The spectral analysis carried out for the previous product (FireCCISFD11) showed that MIRBI and NBR2 spectral indices exhibited highest separability values between burned and unburned categories along with the Near Infrared (NIR) reflectance band (Bastarrika and Roteta, 2018); both indices are derived from two bands located in the Short Wave Infrared (SWIR) region of the spectrum, bands B11 and B12. Since these two bands are acquired at 20 m of spatial resolution, the BA detection by this algorithm is limited to this same resolution, despite Sentinel-2 data containing bands at 10 m in other spectral regions. Therefore, only three spectral bands are used by the algorithm: B8A located in the NIR region (wavelengths 854 – 875 nm), and B11 (1565 – 1658 nm) and B12 (2100 – 2280 nm) SWIR bands, all at 20 m.

Only images acquired by Sentinel-2A (S2A) were used for the FireCCISFD11, since the Sentinel-2B (S2B) was not in operation yet in 2016. This limited the revisit time to 10 days, but this has been improved to 5 days since the second satellite was launched on 7 March 2017. Due to the more frequent revisit time and the larger amount of data, fewer errors were expected for the processing of the FireCCISFD20 product in 2019.

However, some significant issue was found when the original algorithm used for FireCCISFD11 was tested in some sample areas with data from 2019 and both satellites (S2A and S2B). A misregistration smaller than a 20 m pixel had already been observed by a study between different S2A images (Yan et al., 2018), but a more significant spatial shift was found between S2A and S2B images when applying the SFD algorithm. This

	Fire_cci	Ref.:	Fire_cci_D2.1.4_ATBD_SFD_v1.0		
	Algorithm Theoretical Basis	Issue	1.0	Date	03/11/2021
	Document – Small Fires Dataset	Page	9		

shift causes a spectral multi-temporal change similar to that of burned areas, and several pixels are classified as BA between images from different satellites (Figure 1). Another cause for increasing commissions is the misclassification of cloud shadows in the SCL by Sen2Cor, an issue already observed for the first SFD from 2016. Since a higher frequency of images is available with both satellites, the likelihood for commission errors due to cloud shadows is also higher. These two issues – the misregistration and detecting clouds shadows as BA – increased commissions from 22.9% (using only S2A data) to 30.5% (combining both S2A and S2B), when the algorithm was tested in some sample sites and compared with reference perimeters. Therefore, S2A and S2B data cannot be directly compared in this new version of the SFD.

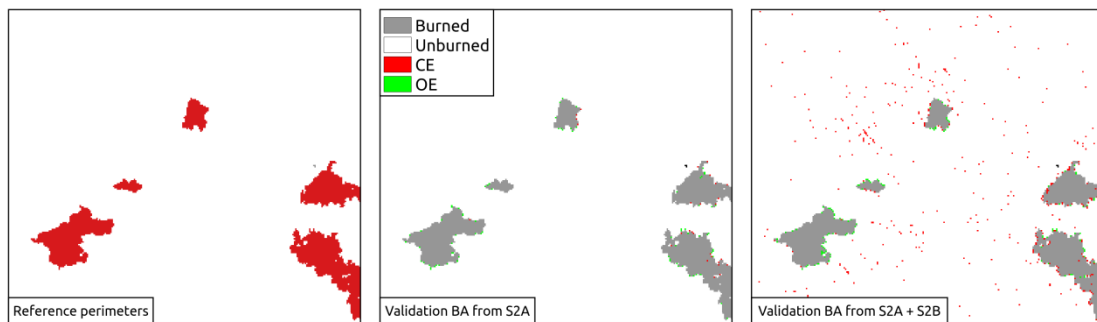


Figure 1. Reference perimeters and validation results, using only S2A data or both S2A and S2B images, in a sample area in tile 36LWN.

5.2 Active fire products

The proposed Sentinel-2 BA algorithm uses the active fire products to check that the spectral/temporal changes detected at the images are due to the fire. While the vector file of Collection 6 MCD14DL hotspots was used for the SFD in 2016 because this was considered the most adequate available product at the time, the Visible Infrared Imaging Radiometer Suite (VIIRS) sensor has been used instead for the SFD in 2019. Both products can be downloaded from the Archive Download Tool (<https://firms.modaps.eosdis.nasa.gov/download/>, last accessed on October 2021). The VIIRS sensor aboard the Suomi-NPP satellite, with its 375-metre resolution, is now available and shows a greater response over fires of relatively small areas due to its better spatial resolution.

5.3 Classification of Burned and Non-Burned Vegetation


5.3.1 Preparation of data

The pre-processing includes all the necessary steps to prepare the input data (Level-2A products after pre-processing at CreoDIAS) so that the algorithm can be applied directly on its output. This includes several phases:

- Spectral index computation.
- Compositing of images for the same date.

5.3.1.1 Spectral indices

Two spectral indices were calculated: the Mid-Infrared Burned Index (MIRBI) and the Normalized Burned Ratio 2 (NBR2), both representing the relation between two very

	fire cci	Fire_cci		Ref.: Fire_cci_D2.1.4_ATBD_SFD_v1.0	
		Algorithm Theoretical Basis		Issue 1.0	Date 03/11/2021
		Document – Small Fires Dataset		Page 10	

important spectral spaces for the burned signal detection: Long SWIR (B12) and Short SWIR (B11). These two spectral indices were selected because they got the highest separability, along with the NIR band, in the spectral analysis carried out before generating the FireCCISFD11 in 2016 (Bastarrika and Roteta, 2018).

The NBR2 and MIRBI spectral index equation is as follows:

$$NBR_2 = \frac{\rho_{SWIRS} - \rho_{SWIRL}}{\rho_{SWIRS} + \rho_{SWIRL}}$$

$$MIRBI = (10 \cdot \rho_{SWIRL} - 9.8 \cdot \rho_{SWIRS} + 2)$$

Where:

- ρ_{SWIRS} = Short Short Wave Infrared Short reflectance [unitless] (B11 band divided by 10000 in the case of Sentinel 2)
- ρ_{SWIRL} = Short Wave Infrared Long reflectance [unitless] (B12 band divided by 10000 in the case of Sentinel 2)

For the NIR, the B8A band was used (divided by 10000 in the case of Sentinel 2).

5.3.1.2 Compositing of scenes of the same date

Some scenes, even if they were acquired in the same orbit at the same time, are split in two different files. This issue is quite easy to detect, as the *Sensing Time Start* and the *Sensing Time Stop* in the products filename is the same. In this case, both images must be joined using the corresponding SCLs as masks, filling the gap of an image (where SCL has the value 0 – NoData) with data from the other image (Figure 2).

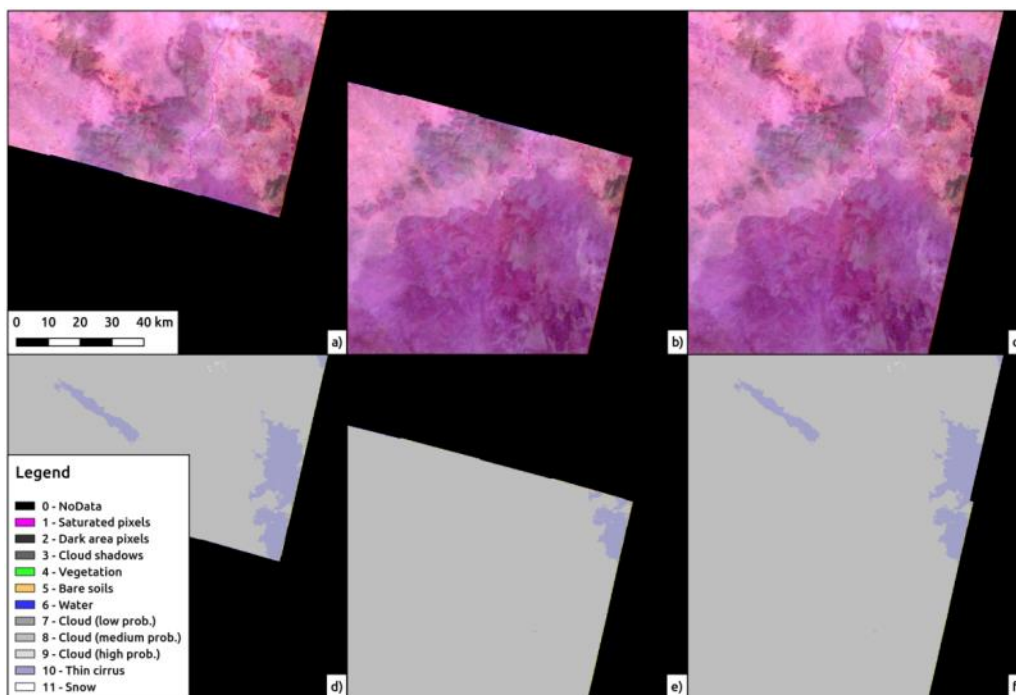


Figure 2. Compositing of two images of the same date in the 33PTK study area of both false colour SWIR2-NIR-Red image and SCL (the right column is the compositing result)

5.3.2 General overview of the BA algorithm

The proposed burned area algorithm compares two Sentinel 2 tiles each time, using 6 variables, the multi-temporal difference $[t] - [t-i]$ and the post values $[t]$ of the MIRBI, NBR2 spectral indices and the NIR, the variables that have shown a higher separability between the burned and not burned category on the spectral analysis carried out before generating the previous FireCCISFD11 product. Due to slight displacements observed between images from different satellites (Sentinel-2A and Sentinel-2B) (Section 5.1), two independent BA products are generated initially, each derived from images acquired by one satellite, and then both products are merged to obtain the final FireCCISFD20 product (see section 5.3.10).

For each product derived from Sentinel-2A or Sentinel-2B data each scene $[t]$ time is compared to the previous four scenes $[t-1, t-2, t-3, t-4]$ in order to complete the areas masked as not burnable in previous images (Figure 3). This criterion means that if $[t-1]$ image is cloud/shadows free, the previous scenes $[t-2, t-3, t-4]$ will not be used. In the current context where using data from only one satellite means a temporal resolution of 10 days (using data from both satellites would have improved the temporal resolution to 5 days), we assume at most going back 40 days as the algorithm defined works better while the compared images are more similar. Our findings have shown high commission errors when comparing scenes older than 40 days in some study areas.

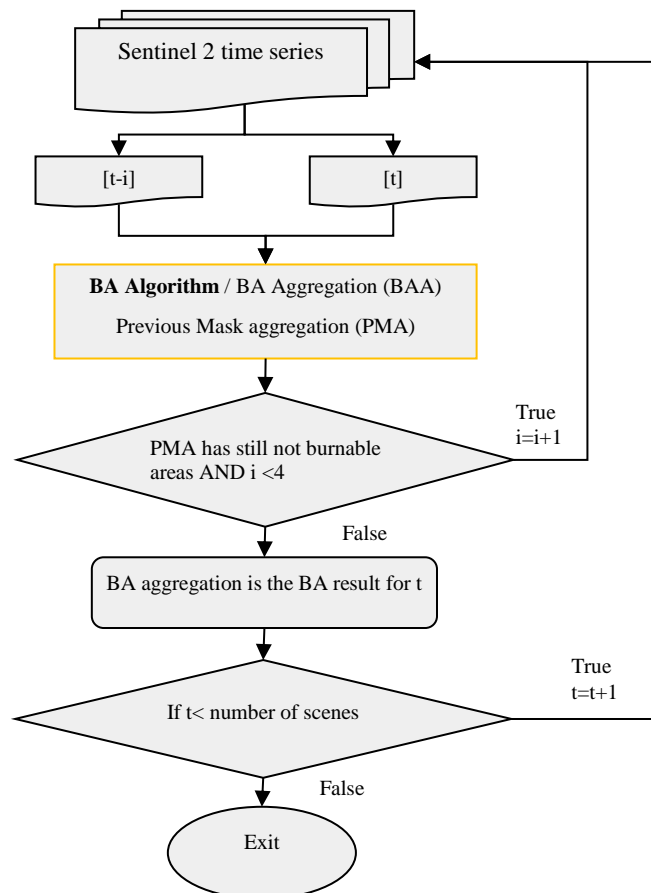



Figure 3. Aggregation process for the Sentinel 2 images from a single satellite

	<p style="text-align: center;">Fire_cci Algorithm Theoretical Basis Document – Small Fires Dataset</p>	Ref.:	Fire_cci_D2.1.4_ATBD_SFD_v1.0			
		Issue	1.0	Date	03/11/2021	
		Page				12

When comparing two scenes the algorithm starts computing the not burnable mask using, both [t] and [t-i] scene classification map (SLC). If the burnable area is below 5 km² or no VIIRS Active Fire Hotspots have been detected in the scene extent during the [t-i, t] interval, the process ends (Figure 4).

If the flow continues, the algorithm starts applying fixed thresholds (see Section 0) for the MIRBI NBR2 and NIR multi-temporal difference, and image based statistics for the MIRBI, NBR2 and NIR [t] images, obtaining the “Initial Burned/Not Burned” – IB and INB- cartography. The initially burned regions, once labelled using a connectivity of 2 (8 neighbour pixels), are crossed with the VIIRS Active Fire hotspots points among the Pre and Post scene dates in order to have a confirmation that those regions are really burned, obtaining the “Initial Burned/Not Burned Confirmed”- IBC and INBC. These hotspots, initially read as vector points, are rasterized to the Sentinel spatial resolution (20m) and dilated to have a 1 km of diameter, the spatial resolution of the original VIIRS active fire product. The BA process ends if no initially burned regions have been confirmed (IBC).

At this point of the algorithm, a two-phase strategy is applied to balance omission and commission errors (Bastarrika, et al., 2011a). Initially Burned Confirmed (BC) based statistics (5th or 95th percentile depending on if the burned signal is higher or lower than the not burned one) are used to set the criteria to establish the seeds, based on the aforementioned 6 variables. The second stage criteria is based exclusively on two variables, the MIRBI and NBR2 multi-temporal difference, where a sigmoid membership function is computed based on IB, INB, IBC, INBC statistics depending on the case (two different options are considered depending on the separability between the confirmed and not confirmed burned areas). The process ends maintaining only the second stage result regions, which have been marked by the seeds.

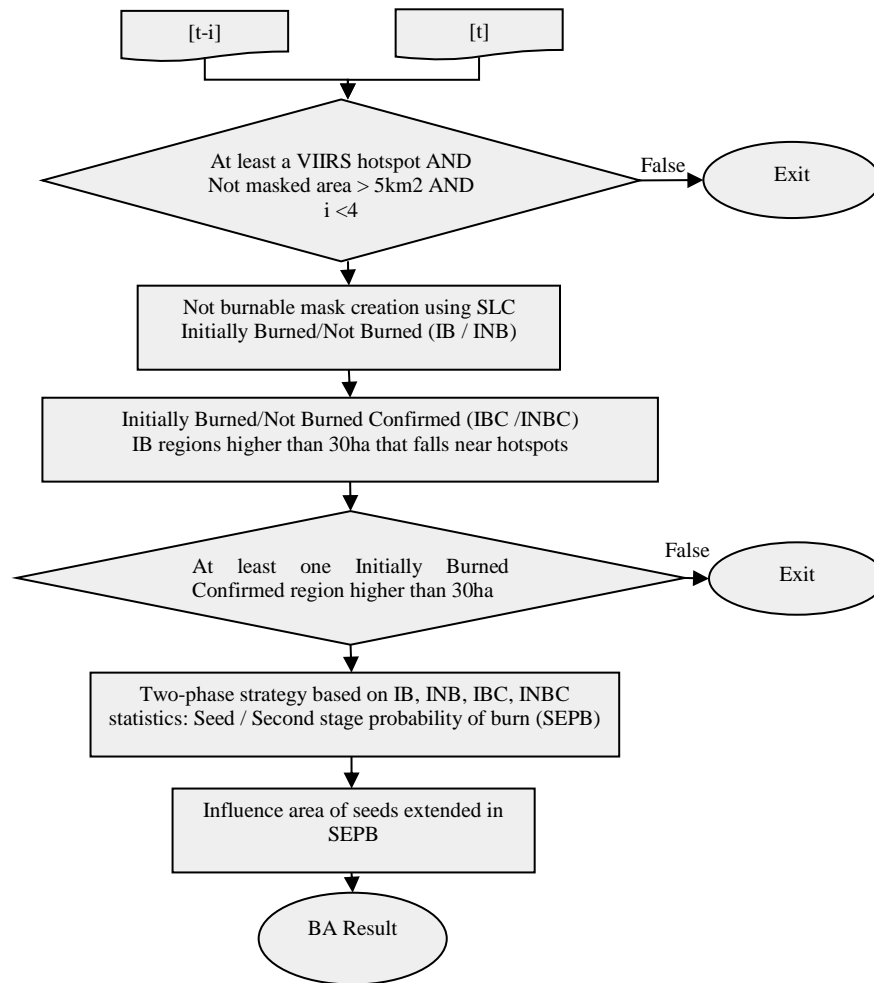



Figure 4. BA algorithm for each pair of Images considered

5.3.3 Not burnable mask

A not burnable mask was defined for each pair of images compared [t-i, t]. A pixel that satisfies any of the following rules was masked (Table 1):

Table 1. Rules applied to obtain the not burnable mask

[t] (Post image)	[t-i] (Previous image)
NO_DATA(0)	NO_DATA(0)
SATURATED_OR_DEFECTIVE (1)	SATURATED_OR_DEFECTIVE (1)
WATER (6)	WATER (6)
CLOUD_MEDIUM_PROBABILITY (8) with a dilation of 5 pixels	CLOUD_MEDIUM_PROBABILITY (8) with a dilation of 5 pixels
CLOUD_HIGH_PROBABILITY (9) with a dilation of 5 pixels	CLOUD_HIGH_PROBABILITY (9) with a dilation of 5 pixels
THIN_CIRRUS (10) with a dilation of 5 pixels	with a dilation of 5 pixels
SNOW (11)	SNOW (11)
Long SWIR (B12) < 0.07	

	Fire_cci		Ref.: Fire_cci_D2.1.4_ATBD_SFD_v1.0
	Algorithm Theoretical Basis		Issue 1.0 Date 03/11/2021
	Document – Small Fires Dataset		Page 14

Summarizing, in addition to not valid data (No data, saturated-defective), Medium-High probability clouds and cirrus with a dilation of 5 pixels (100 metres) are used in order to have a more reliable cloud mask, applied to the image pair considered. Low probability clouds are not used because as previously said, it would be masked a very significant quantity of burned areas. The “dark areas” are not masked for the same reason, and the Long SWIR band (B12) criteria is used, only in the Post image, where in general burned areas and shadows show a good separability (lower values for cloud shadows and higher for burned ones).

When only a reduced surface is observed between a pair of images, a considerable proportion of initially burned pixels (from the next step) can actually be cloud shadows, and the final burned areas will be estimated from wrong statistics extracted from those initially burned pixels. To avoid this, a pair of images will be processed only if there are at least 5 km² (12500 pixels) not burnable; this is an attempt to avoid wrong burned statistics. All the statistics computed in the next sections do not use the not burnable masked pixel values.

5.3.4 Initially Burned/Not Burned Area detection (IB/INB)

The initialization of the algorithm is crucial and it is based on the spectral analysis made before the previous SFD, where NBR2, MIRBI and NIR multi-temporal difference variables showed higher spectral separability between burned and unburned categories. Values dividing these two categories best are used as fixed thresholds. A pixel will be labelled as initially burned (IB/INB) if it satisfies the next 7 rules in Table 2.

The aim behind this first initialization is double. On one hand, to have burned candidates that will be crossed with the active fires, when they will become Initially Burned Confirmed (IBC). On the other hand, to obtain a good identification of the not burned background that will be used as comparison surface at the refinement process.

Table 2. Rules applied to obtain the Initially Burned Result

Rule number	Criteria
1	$MIRBI_t > \text{mean}(MIRBI_t)$
2	$(MIRBI_t - MIRBI_{t-i}) > 0.25$
3	$NBR2_t < \text{mean}(NBR2_t)$
4	$(NBR2_t - NBR2_{t-i}) < -0.05$
5	$NIR_t < \text{mean}(NIR_t)$
6	$NIR_t - NIR_{t-i} < -0.01$
7	Not masked

NOTE: To compute the mean of the post fire (t) data, only data that are not masked are used

5.3.5 Initially Burned (Not) Confirmed (IBC/IBNC)

The IB pixels were crossed with the VIIRS derived hotspots, in order to obtain a confirmation that the spectral change detected on the previous step is due to the fire. For doing that, the IB pixels were labelled in regions (using a connectivity of 2, considering 8 neighbour pixels), and only the regions higher than 30 ha (750 pixels in Sentinel 2) were used to be checked by the active fires. Note that the active fires detections are derived from a resolution of 375 m², which is equivalent to approximately 350 Sentinel 2 pixels.

To take into account the spatial disagreement among the active fire and Sentinel 2 detection, a dilation of 19 pixels (380 m of diameter) was applied to the active fire points rasterized in the Sentinel 2 resolution (20m) from the shapefile. Only the hotspots detected among the Previous [t-i] and Post [t] and located in the tile extent were considered.

5.3.6 Burned seeds

To compute the burned seeds, basic statistics derived from the Initially Burned Confirmed regions are used, specifically the 5th percentile for the variables whose burned values are higher than the not burned ones, and the 95th percentile for the opposite case. A pixel will be labelled as seed if it satisfies all 7 rules in Table 3.

Table 3. Rules applied to obtain Burned Seeds

Rule number	Criteria
1	$MIRBI_t > 5^{th_Percentile_IBC}(MIRBI_t)$
2	$(MIRBI_t - MIRBI_{t-1}) > 5^{th_Percentile_IBC}(MIRBI_t - MIRBI_{t-1})$
3	$NBR2_t < 95^{th_Percentile_IBC}(NBR2_t)$
4	$(NBR2_t - NBR2_{t-1}) < 95^{th_Percentile_IBC}(NBR2_t - NBR2_{t-1})$
5	$NIR2_t < 95^{th_Percentile_IBC}(NIR_t)$
6	$NIR_t - NIR_{t-1} < 95^{th_Percentile_IBC}(NIR_t - NIR_{t-1})$
7	Not masked

5.3.7 Second Stage Probability of Burn (SEPB)

For the refinement process, two behaviours were considered. To choose one over the other option, the separability between the IBC regions and the IBNC classes were computed for the three multi-temporal variables ($MIRBI_t - MIRBI_{t-i}$, $NBR2_t - NBR2_{t-i}$, $NIR_t - NIR_{t-i}$) using the M separability index:

$$M = \frac{abs(\mu_{IBC} - \mu_{IBNC})}{\sigma_{IBC} + \sigma_{IBNC}}$$

Where

μ_{IBC} = Mean of the variable for the Initially Burned Confirmed category

σ_{IBC} = Standard deviation for the Initially Burned Confirmed category

μ_{IBNC} = Mean of the variable for the Initially Burned Not Confirmed category

σ_{IBNC} = Standard deviation for the Initially Burned Not Confirmed category

The aim behind this separability choice was to assess if the regions confirmed as burned by hotspots differ spectrally from those that have not been confirmed. A threshold of 1.0 is usually used to decide whether two categories are separable, but here a 0.75 value was chosen to assure that IBC and IBNC pixels are spectrally similar. Two cases are considered:

- a) If one of the following conditions is satisfied: $M_{MIRBI_t - MIRBI_{t-i}} > 0.75$ OR $M_{NBR2_t - NBR2_{t-i}} > 0.75$ OR $M_{NIR_t - NIR_{t-i}} > 0.75$
- b) If the three conditions are satisfied (Not a) case): $M_{MIRBI_t - MIRBI_{t-1}} < 0.75$ AND $M_{NBR2_t - NBR2_{t-1}} < 0.75$ AND $M_{NIR_t - NIR_{t-1}} < 0.75$

The refinement process for both cases is based on MIRBI multi-temporal difference and NBR2 multi-temporal difference variables. The main idea is to establish a threshold value dependent on the ‘not burned’ background and already detected burned areas, using the 90th percentile of not burned background pixels as the minimum value and the 50th percentile of burned pixels as the maximum value of a membership function.

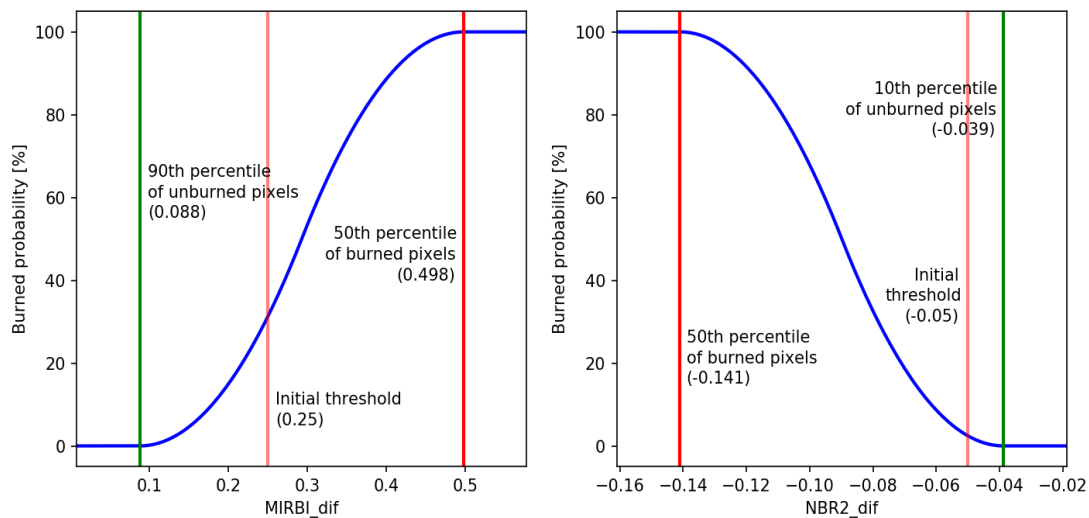


Figure 5. s-shape and z-shape sigmoid membership functions applied to MIRBI and NBR2 temporal differences, in tile 28PET between December 22 2015 and January 11 2016.

A sigmoid curve (s-shaped for MIRBI and z-shaped for NBR2) (Figure 5) is used to define the burned membership function so that the transition between both categories is more continuous. The minimum and maximum values for this function are extracted from not burned background and burned areas, depending on the case and following the next equations:


- a) IBC and IBNC pixels differ significantly, so IBNC is used as not burned background for the statistics (along with INB), and only IBC as burned.

$$MIRBI_{burned_membership} = scurve(90th_Percentile_IBNC_INB(MIRBI_t - MIRBI_{t-i}), 50th_Percentile_IBC(MIRBI_t - MIRBI_{t-i}))$$

$$NBR2_{burned_membership} = zcurve(10th_Percentile_IBNC_INB(NBR2_t - NBR2_{t-i}), 50th_Percentile_IBC(NBR2_t - NBR2_{t-i}))$$

where:

- *scurve*: is the sigmoid s-shape membership function
- *zcurve*: is the sigmoid z-shape membership function
- *90th_Percentile_IBNC_INB*: 90th percentile of those areas labelled as Initially Not Burned or Initially Burned Not Confirmed
- *10th_Percentile_IBNC_INB*: 10th percentile of those areas labelled as Initially Not Burned or Initially Burned Not Confirmed
- *50th_Percentile_IBC*: 50th percentile of those areas labelled as Burned on the Initially Burned Confirmed stage

	Fire_cci	Ref.:	Fire_cci_D2.1.4_ATBD_SFD_v1.0		
	Algorithm Theoretical Basis	Issue	1.0	Date	03/11/2021
	Document – Small Fires Dataset	Page			17

b) IBC and IBNC pixels have similar values, so only INB is used as not burned background, and both IBC and IBNC as burned.

$$MIRBI_{burned_membership} = \text{scurve}(90th_Percentile_INB(MIRBI_t - MIRBI_{t-1}), 50th_Percentile_IBC_IBNC(MIRBI_t - MIRBI_{t-1}))$$

$$NBR2_{burned_membership} = \text{zcurve}(10th_Percentile_INB(NBR2_t - NBR2_{t-1}), 50th_Percentile_IBC_IBNC(NBR2_t - NBR2_{t-1}))$$

where:

- *scurve*: is the sigmoid s-shape membership function
- *zcurve*: is the sigmoid z-shape membership function
- *90th_Percentile_INB*: 90th percentile of those areas labelled as not burned on the initialization stage
- *10th_Percentile_INB*: 10th percentile of those areas labelled as not burned on the initialization stage
- *50th_Percentile_IBC_IBNC*: 50th percentile of those areas labelled as burned on the initialization stage

These membership functions are used as burned probability functions based on MIRBI and NBR2 temporal differences. The multiplication of both probability functions, called Second Stage Probability of Burn (SEPB), is used as the probability of burn for the final result. This lowers the probability values, but it is necessary because both spectral indices are independent variables. This is also why the recommended threshold of the final product between unburned and burned classes is so low.

$$SEPB = MIRBI_{burned_membership} \cdot NBR2_{burned_membership}$$

5.3.8 Probability of burn results

The burned seeds were applied in the Second Stage Probability of Burn image for the final result. Seeds were typically used in images with discrete values (rather binary values), as only patches containing a seed were selected removing areas with no seed. However, as the SEPB image is a continuous variable, a different approach is used in this case.

The probability of a pixel being burned (P_b) of the final result for each pixel is the highest threshold that can be used in the SEPB to classify burned and unburned areas, so that the pixel in question is part of a burned area containing a seed. That is to say, if a higher threshold than the P_b of a pixel is applied, the pixel will be part of a patch (using the connectivity of 2, considering 8 neighbour pixels) that does not contain any seed and classified as not burned; otherwise it will be connected to a burned area containing a seed, and it will be classified as a burned pixel. In Figure 6, results of using several thresholds are shown. The P_b value that connects the seed to the pixel group in the northeast of the red ellipse is found by decreasing the threshold levels; this threshold value is then applied to that group of pixels ($P_b=66\%$).

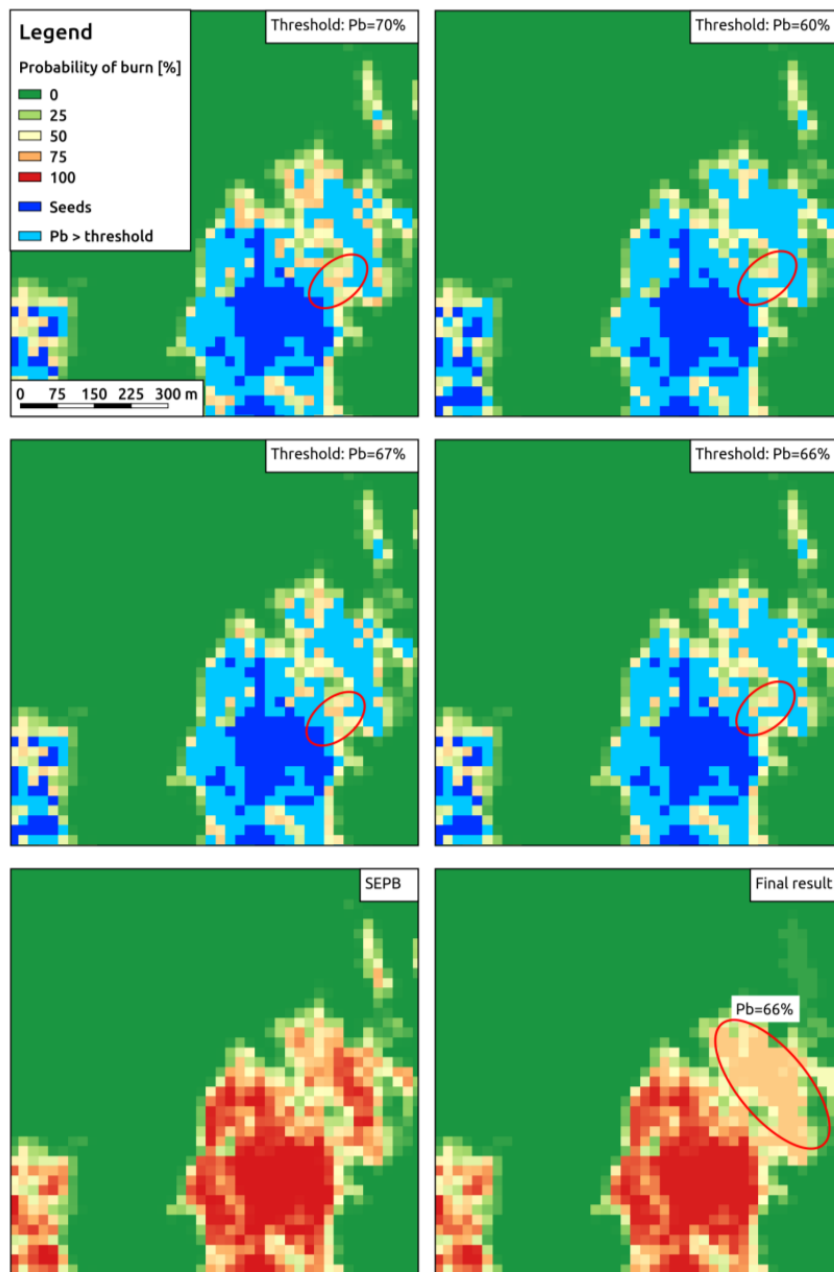


Figure 6. Extension of seeds' influence area in the SEPB for a sample zone of the 30PWQ study area, between 27th December 2015 and 6th January 2016; the legend is the same for all the maps.

5.3.9 Resampling of the Probability of burn

The resulting layer of the algorithm has continuous values from 0 to 100 indicating the probability of burn of the pixel, but the user of the product may prefer a binary layer with two categories for unburned and burned areas. A threshold of 50% is typically used in these cases, but a lower value should be used in this product due to the following reasons:

- When generating sigmoid curves in the refinement process (section 5.3.7) the percentiles for burned and unburned categories are not symmetric, being the sigmoid curve closer to the burned class than to the unburned one, and thus causing the boundary between both classes to be in a lower probability value.

- The probability value of the SEPB is obtained by multiplying MIRBI and NBR2 probability functions, lowering even more the threshold value.

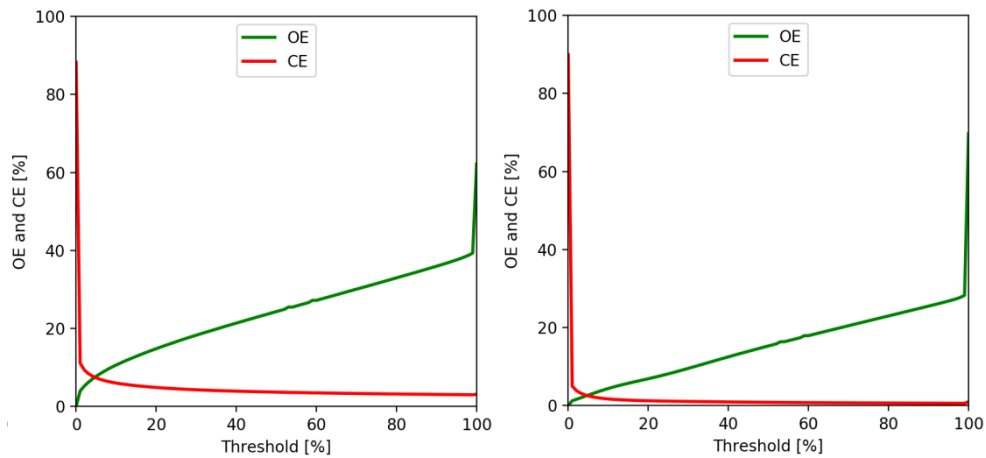


Figure 7. Evolution of omission and commission errors depending on the threshold in two sample tiles (31PEN to the left and 34PET to the right).


In order to decide which the best threshold was, the evolution of both omissions and commissions was analysed depending on the applied threshold. As it is shown in Figure 7, this threshold is around the 5% value. Since this value could be confusing for the product’s users, the probability values were rescaled so that this original 5% value would become the common 50% threshold, following Table 4. Due to the scale of the values being rescaled, the new probability values have discrete values in intervals of 10%. As pixels with a probability of burn below 50% are considered as not burned, only pixels above this threshold are represented in the final SFD product.

Table 4. Lookup Table for the rescaling process.

Original probability	Rescaled probability (discrete values)
% 0	% 0
% 1	% 10
% 2	% 20
% 3	% 30
% 4	% 40
% 5-14	% 50
% 14-23	% 60
% 23-32	% 70
% 32-41	% 80
% 41-50	% 90
> =%50	% 100

5.3.10 Merging of Sentinel-2A and -2B

As explained in section 5.1, BA detected with data from both satellites (BAS2A-B) contained a significant increase of commissions, due to a misregistration issue found when comparing images from different satellites. Therefore, two independent BA products are created up to this point, one based exclusively on images acquired by the

	Fire_cci		Ref.:	Fire_cci_D2.1.4_ATBD_SFD_v1.0		
	Algorithm Theoretical Basis		Issue	1.0	Date	03/11/2021
	Document – Small Fires Dataset		Page	20		

Sentinel-2A satellite (BAS2A), the other on Sentinel-2B images (BAS2B). Both products are then merged into the final FireCCISFD20 product.

Both BA products (BAS2A and BAS2B) are composed by several images with P_b values resulting from the previous step of the algorithm; each image corresponds to an acquisition date by the corresponding S2A or S2B satellite, ideally one image every 10 days. The merging methodology consists in comparing every P_b image in one product with the closest previous and following images in the other product, and removing BA that was not detected by both products. This can be seen in Figure 8, where a sample date from November 26, belonging to the BAS2A product, is shown. Every burned pixel in this P_b image is compared with the closest P_b images in BAS2B, and burned pixels from November 26 are removed if they were not detected as burned in either the previous image to that date in BAS2B, or in the first available image of BAS2B posterior to November 26. In this way, most of the detected BA, which was actually commission error due to cloud shadows, does not appear in the final product.

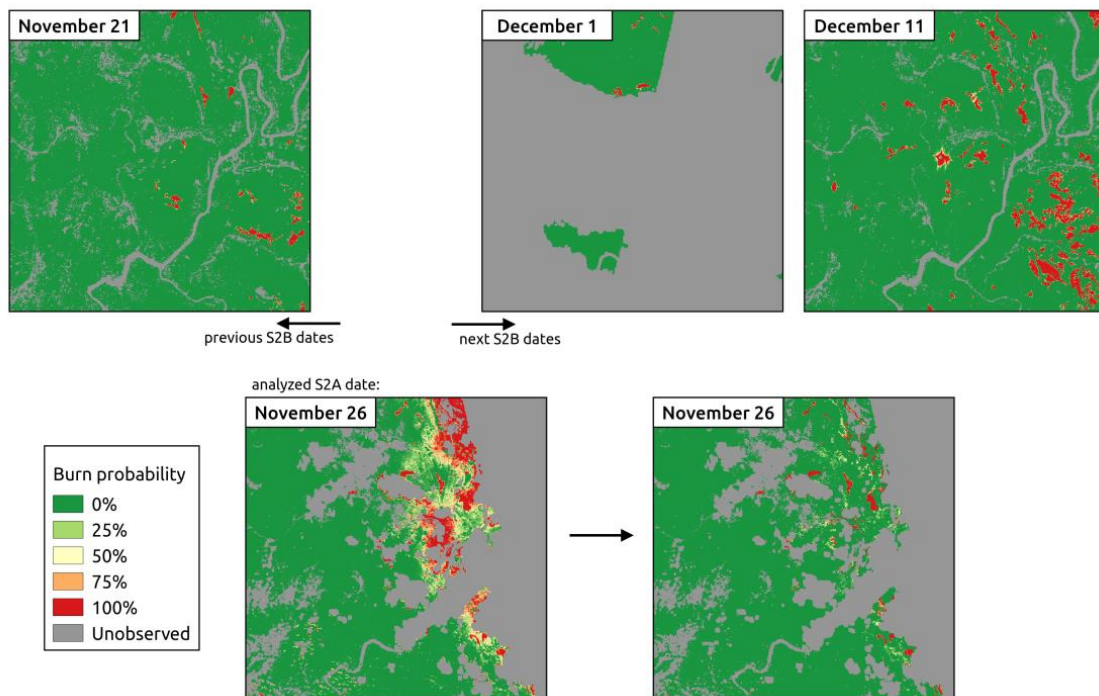


Figure 8. Comparison of a BAS2A P_b image with closest previous and next BAS2B images, and removal of BA that were not detected by BAS2B.

This methodology for merging both products avoids the aforementioned issues that increased commissions (misregistration and errors due to cloud shadows), since commission-error areas remain only if they were detected by both BAS2A and BAS2B products. This is shown in Figure 9, where large areas actually corresponding to shadows were classified as BA by BAS2A. Since these shadows were observed on an image acquired by the S2A satellite, the BAS2B product did not contain this error, but would have appeared in the final product if images from both satellites were combined straightaway (BAS2A-B). However, producing two separate BA products and merging them later removes these commissions, as it can be seen in the final FireCCISFD20 product.

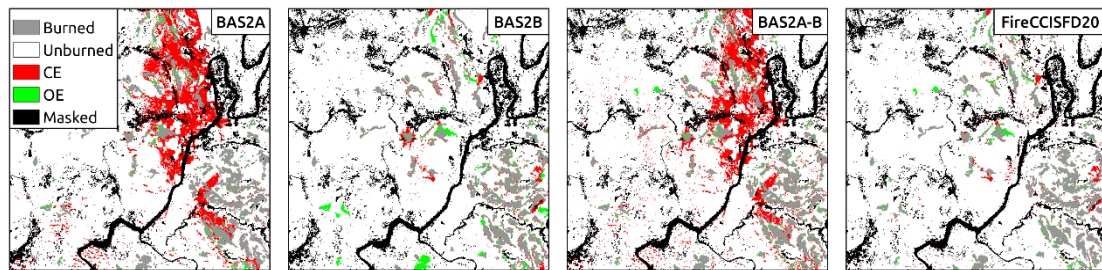


Figure 9. Comparison of errors depending on the datasets used or how these datasets are combined, in the same sample area as Figure 8.

6 Results of Test over the study areas

Quality assessment of the S2 algorithm was based on 26 test sites selected by stratified random sampling (Padilla et al., 2017). Sampling units were S2 tiles, with one available cloud-free image every 20 days during a period at least 2-months long. These long sampling units were assigned the predominant Olson biome (Olson et al., 2001), and low/high fire activity based on the number of VIIRS active fires. The 26 test sites were then randomly selected from these 14 strata, proportionally to the mean BA in each stratum; these are shown in Figure 10. Reference perimeters at each site were created between every pair of consecutive images, in a $20 \times 20 \text{ km}^2$ window at the centre of the MGRS tile, and derived from S2 data at 10 m of spatial resolution. The RP tool from BAMT based on a supervised classification (Roteta et al., 2021) was used for reference perimeter creation.

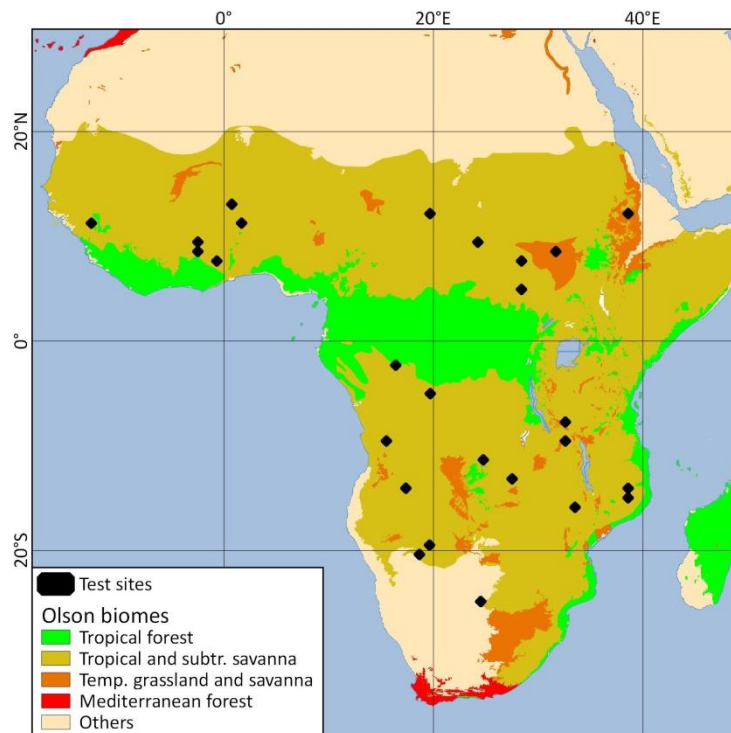



Figure 10. Location of the 26 test sites and major Olson biomes.

Table 5 shows the results of the algorithm in the 26 test sites and the aggregated results for the whole dataset. Omissions are higher than commissions (13.5% and 7.8%, respectively, for the whole dataset). Commissions are mainly related to cloud borders

(clouds not classified by Sen2Cor and so not masked) and to a lesser detection of burned areas, especially around active fires where BA are overestimated; highest commission errors correspond to study areas where there were only small burned areas but many agricultural fields with similar spectral signal to burned areas. On the other hand, omissions are caused by either too strict thresholds or by the absence of hotspots (no BA is classified when no active fire can be found in the tile between pre- and post-fire dates).

Table 5. Quality assessment of the SFD algorithm in the 26 test areas.

Tile	First date	Last date	BA [km ²]		OE [%]	CE [%]	DC [%]
			Reference data	Algorithm results			
28PGT	20190102	20190527	311.8	319.9	11.5	13.7	87.4
30NYP	20190102	20190313	874.0	798.5	15.8	7.9	88.0
30PWQ	20191116	20191231	968.7	995.5	3.4	6.0	95.3
30PWR	20190110	20190420	94.8	38.2	69.3	23.8	43.7
31PBQ	20190117	20190407	1.4	0.5	82.1	44.0	27.1
31PCN	20191016	20191230	1062.8	1039.3	3.5	1.3	97.6
33LWK	20190418	20190920	1438.4	1443.5	2.5	2.8	97.3
33LYE	20190430	20191106	1000.7	1036.4	2.7	6.1	95.6
33MXT	20190607	20190831	250.6	204.2	27.3	10.8	80.1
34JHT	20190103	20191219	0.0	0.0	0.0	0.0	100.0
34KBC	20190107	20191213	0.0	0.0	0.0	0.0	100.0
34KCD	20190124	20191210	59.1	57.6	8.7	6.3	92.5
34MCV	20190609	20190917	253.7	157.2	59.7	34.9	49.8
34PCU	20190113	20190428	10.2	9.3	18.5	10.2	85.4
34PHR	20191029	20191228	788.2	543.3	37.6	9.5	73.8
35LKH	20190501	20191102	1037.5	1120.0	5.0	12.0	91.4
35LNF	20190503	20191109	1109.8	1013.1	16.5	8.6	87.3
35NPF	20190106	20190312	757.0	699.9	24.0	17.8	79.0
35NPJ	20190923	20191227	906.0	830.8	16.1	8.4	87.6
36LVQ	20190417	20191113	1059.3	1099.7	8.0	11.4	90.3
36LWH	20190708	20191105	909.4	863.3	12.0	7.3	90.3
36MVS	20190522	20191014	1380.4	1410.6	3.3	5.3	95.7
36PUQ	20190103	20190403	654.9	649.3	1.7	0.8	98.7
37LDE	20190523	20191119	1338.3	1090.3	21.2	3.3	86.9
37LDD	20190801	20191204	853.2	632.3	37.5	15.7	71.8
37PDP	20190815	20191228	0.1	0.0	75.6	3.0	39.0
Aggregated results			17120.4	16052.4	13.5	7.8	89.3

	Fire_cci		Ref.:	Fire_cci_D2.1.4_ATBD_SFD_v1.0		
	Algorithm Theoretical Basis		Issue	1.0	Date	03/11/2021
	Document – Small Fires Dataset		Page	23		


7 Limitations of the product

The limitations found in the S2 processing and algorithm development are:

1. Dependence on VIIRS hotspots: The algorithm presented in this document depends totally on hotspots from the VIIRS active fire product, generated by detection of thermal anomalies. The lack of hotspots in a tile between pre- and post-fire dates or no hotspot being closer than 180m to IB (Initially Burned) areas means that no burned area is detected in the outcome of the algorithm. This leads to a 100% omission error even if there were some small areas burned in this period. This is, however, an improvement in comparison with the previous FireCCISFD11 product, for which VIIRS active fires were not available yet and MODIS hotspots at coarser resolution (1 km) were used instead.
2. Confidence information: The result of the outcome indicates the probability of burn for every pixel with a value between 0% and 100% (not burned and burned, respectively), being this probability function extracted from IBC (Initially Burned Confirmed, IB areas crossed with hotspots) areas. However, the initialization of the algorithm is based in thresholds derived from initial spectral analyses, so the probability values are not totally dependent on image characteristics.

8 References

- Bastarrika, A., Alvarado, M., Artano, K., Martinez, M., Mesanza, A., Torre, L., Ramo, R., & Chuvieco, E. (2014). BAMS: A Tool for Supervised Burned Area Mapping Using Landsat Data. *Remote Sensing*, 6, 12360-12380.
- Bastarrika, A., Chuvieco, E., & Martin, M.P. (2011a). Automatic Burned Land Mapping From MODIS Time Series Images: Assessment in Mediterranean Ecosystems. *IEEE Transactions on Geoscience and Remote Sensing*, 49, 3401-3413.
- Bastarrika, A., Chuvieco, E., & Martín, M.P. (2011b). Mapping burned areas from Landsat TM/ETM+ data with a two-phase algorithm: balancing omission and commission errors. *Remote Sensing of Environment*, 115, 1003-1012.
- Bastarrika A. & Roteta E. (2018) ESA CCI ECV Fire Disturbance: D2.1.2 Algorithm Theoretical Basis Document-SFD, version 1.0. Available at: <https://climate.esa.int/en/projects/fire/key-documents/>
- Boschetti, L., Roy, D.P., Justice, C.O., & Humber, M.L. (2015). MODIS–Landsat fusion for large area 30m burned area mapping. *Remote Sensing of Environment*, 161, 27-42.
- Chuvieco, E., Martín, M.P., & Palacios, A. (2002). Assessment of different spectral indices in the red-near-infrared spectral domain for burned land discrimination. *International Journal of Remote Sensing*, 23, 5103-5110.
- Chuvieco, E., Yue, C., Heil, A., Mouillot, F., Alonso-Canas, I., Padilla, M., Pereira, J.M., Oom, D., & Tansey, K. (2016). A new global burned area product for climate assessment of fire impacts. *Global Ecology and Biogeography*, 25, 619-629.
- Chuvieco, E., M.L. Pettinari, A. Heil and T. Storm (2017) ESA CCI ECV Fire Disturbance: Product Specification Document, version 6.3. Available at: <http://www.esa-fire-cci.org/documents>

	fire cci	Fire_cci		Ref.: Fire_cci_D2.1.4_ATBD_SFD_v1.0	
		Algorithm Theoretical Basis		Issue 1.0	Date 03/11/2021
		Document – Small Fires Dataset		Page 24	

Drusch, M., Del Bello, U., Carlier, S., Colin, O., Fernandez, V., Gascon, F., Hoersch, B., Isola, C., Laberinti, P., & Martimort, P. (2012). Sentinel-2: ESA's optical high-resolution mission for GMES operational services. *Remote Sensing of Environment*, 120, 25-36.

Giglio, L., Loboda, T., Roy, D.P., Quayle, B., & Justice, C.O. (2009). An active-fire based burned area mapping algorithm for the MODIS sensor. *Remote Sensing of Environment*, 113, 408-420.

Giglio, L., Randerson, J.T., & Werf, G.R. (2013). Analysis of daily, monthly, and annual burned area using the fourth generation global fire emissions database (GFED4). *Journal of Geophysical Research: Biogeosciences*, 118, 317-328.

GCOS (2016). *The Global Observing System for Climate: Implementation Needs*. Geneva, Switzerland: GCOS-200. World Meteorological Organization.

Hantson, S., Padilla, M., Corti, D., & Chuvieco, E. (2013). Strengths and weaknesses of MODIS hotspots to characterize global fire occurrence. *Remote Sensing of Environment*, 131, 152-159.

Olson, D. M., E. Dinerstein, E. D. Wikramanayake, N. D. Burgess, G. V. N. Powell, E. C. Underwood, J. A. D'Amico, I. Itoua, H. E. Strand, J. C. Morrison, C. J. Loucks, T. F. Allnutt, T. H. Ricketts, Y. Kura, J. F. Lamoreux, W. W. Wettengel, P. Hedao and K. R. Kassem (2001). *Terrestrial Ecoregions of the World: A New Map of Life on Earth*. *BioScience* 51: 933-938.

Padilla, M., Stehman, S.V., Hantson, S., Oliva, P., Alonso-Canas, I., Bradley, A., Tansey, K., Mota, B., Pereira, J.M., & Chuvieco, E. (2015). Comparing the Accuracies of Remote Sensing Global Burned Area Products using Stratified Random Sampling and Estimation. *Remote Sensing of Environment*, 160, 114-121.

Padilla, M., Olofsson, P., Stehman, S.V., Tansey, K., & Chuvieco, E. (2017). Stratification and simple allocation for reference burned area data. *Remote Sensing of Environment*, 203, 240-255.

Randerson, J., Chen, Y., Werf, G., Rogers, B., & Morton, D. (2012). Global burned area and biomass burning emissions from small fires. *Journal of Geophysical Research: Biogeosciences* (2005–2012), 117 - G04012, 1-23.

Roteta, E., Bastarrika, A., Padilla, M., Storm, T., & Chuvieco, E. (2019). Development of a Sentinel-2 burned area algorithm: Generation of a small fire database for sub-Saharan Africa. *Remote Sensing of Environment*, 222, 1-17.

Roteta, E., Bastarrika, A., Franquesa, M., & Chuvieco, E. (2021). Landsat and Sentinel-2 Based Burned Area Mapping Tools in Google Earth Engine. *Remote Sensing*, 13, 816.

Roy, D., & Landmann, T. (2005). Characterizing the surface heterogeneity of fire effects using multi-temporal reflective wavelength data. *International Journal of Remote Sensing*, 26, 4197-4218.

Yan, L., Roy, D.P., Li, Z., Zhang, H.K., & Huand, H. (2018). Sentinel-2A multi-temporal misregistration characterization and an orbit-based sub-pixel registration methodology. *Remote Sensing of Environment*, 215, 495-506.

Zhu, Z., & Woodcock, C.E. (2014). Automated cloud, cloud shadow, and snow detection in multitemporal Landsat data: An algorithm designed specifically for monitoring land cover change. *Remote Sensing of Environment*, 152, 217-234.

Annex: Acronyms and abbreviations

AD	Applicable Document
ATBD	Algorithm Theoretical Basis Document
BA	Burned Area
BAMT	Burned Area Mapping Tools
BOA	Bottom of Atmosphere
CCI	Climate Change Initiative
ESA	European Space Agency
ECV	Essential Climate Variables
GCOS	Global Climate Observing System
GHG	Green House Gases
IBC	Initially burned confirmed
IB	Initially burned
INB	Initially not burned
INBC	Initially not burned confirmed
IPCC	Intergovernmental Panel on Climate Change
L1C	Level-1C
L2A	Level-2A
MGRS	Military Grid Reference System
MIRBI	Mid-Infrared Burned Index
MODIS	Moderate Resolution Imaging Spectroradiometer
MSI	Multi Spectral Instrument
NBR2	Normalized Burned Ratio 2
NIR	Near InfraRed
OLI	Operational Land Imager
S2	Sentinel-2
S2A	Sentinel-2A
S2B	Sentinel-2B
SCL	Scene CLasification
SEPB	Second Stage Probability of Burn
SFD	Small Fire Dataset
SWIR	ShortWave Infra Red
TOA	Top of Atmosphere
USGS	United States Geological Survey
UTM	Universal Transverse Mercator
VIIRS	Visible Infrared Imaging Radiometer Suite